

Coastal Erosion from Space



Algorithm Theoretical Baseline Document

Ref: SO-TR-ARG-003-055-009-ATBD-GL

Date: 10/08/2022

Customer: ESA

Contract Ref.: 4000126603/19/I-LG





This page is intentionally left blank



Version and Signatures

Version	Date	Modification
	09/12/2019	Review
Verification by	François-Regis Martin-Lauzer	
Authorisation	Craig Jacobs	

Acronyms

ARCSI: Atmospheric and radiometric correction of satellite imagery

AROSICS: Automated and Robust Open-Source Image Coregistration Software

CDOM: Coloured dissolved organic matter

CNES: Centre national d'études spatiales (Fr)

DEM: Digital elevation model

DoD: DTM of difference

DSI: Datum-based shoreline indicators

DTM: Digital terrain model

EO: Earth observation

GRD: Ground range detected

HR: High resolution

ICZM: Integrated Coastal Management

IDA: Image data analysis

IOPs: Inherent optical properties

MSI: Multi-spectral imager

NIR: Near infra-red

OLI: Operational land imager

SAR: Synthetic-aperture radar

SDB: Satellite derived bathymetry

TBDEM: Topo-bathymetric digital elevation model

URD: User requirement document

VHR: Very high resolution



Applicable and reference documents

Id	Description	Reference
AD-1	Requirement Baseline Document	SO-RP-ARG-003-055-006-RBD_v1.0_20190916



Contents

Version and Signatures	1
Acronyms	2
Applicable and reference documents	3
Contents	4
List of Figures	5
List of Tables	6
3 Overview and Background Information	7
3.3 Product Requirement	7
3.4 Feasibility Study	7
3.5 Product Specifications	13
4 Algorithm Description	14
4.3 Processor Design	16
4.4 Processor Overview	18
4.5 Data Requirements	20
5 Theoretical Description of the Model	20
5.1 Physical Description	20
5.2 Algorithm Performance Estimates	23
5.3 Products Validation	25
6 Refactoring	30
6.3 Verification	30
6.4 Processing Time Improvement	31
6.5 Metadata	32
7 Conclusion	33
8 References	34

List of Figures

Figure	Description	Page
Figure 2.1:	(A) Reference image subset (Landsat-8, band 5), small figure demonstrates full extent; (B) target image (RapidEye-5, band 5); (C) calculated tie point grid before correction (absolute shift vector length in metres) including false-positives; and (D) -----	14
Figure 2.2.	Flow chart of AROSICS (Scheffler et al., 2017) -----	15
Figure 2.3.	Possible scenarios for HR coregistration -----	17
Figure 2.4:	Schematic overview of the geolocation processing module -----	19
Figure 2.5.	Schematic workflow for coregistering a stack of HR targets to a single VHR -----	19
Figure 3.1:	Subset images within the matching window in spatial and frequency domains and the -----	21
Figure 3.2.	Summary of example satellite datasets -----	23
Figure 3.3.	Distribution of detected geometric shifts before and after correction. RMSE in pixel units always refers to the spatial resolution during image matching: (A,B) use case INTER1—Sentinel-2/Landsat-8; (C,D) use case INTER2—RapidEye-5/Landsat-8; and (E,F)-----	24
Figure 3.4.	top: image large scale bottom: Zoom), -----	24
Figure 3.5.	Equation for SSIM index-----	25
Figure 3.6.	Quality control (level of validation)-----	26
Figure 3.7.	Analysis of the SIM index (before and after) the coregistration for two different dates-----	27
Figure 3.8.	Coregistration quantification -----	28
Figure 3.9.	SSIM Index comparison before and after the Coregistration process -----	28
Figure 3.10.	Correlation study of the SSIM index between the 2016 and 2018 image -----	29
Figure 4.1.	Italy T33TUL. Original coregistered polygon in red and refactored version in blue -----	30
Figure 4.2.	Italy T33SWB. Original coregistered polygon in red and refactored in blue-----	31



List of Tables

Table 1. EO missions and their specifications with optical sensors -----	9
Table 2. AROSICS parameters for each level of processing -----	18
Table 3. SSIM comparison pre and post coregistration -----	27
Table 4. SSIM comparison at the 90th percentile-----	31
Table 5. Coregistration processing times -----	32
Table 6. Metadata produced for each coregistered product -----	32

1 Overview and Background Information

1.1 Product Requirement

One of the key innovative requirements that has been placed upon this project is to provide a level of accuracy that is placed upon each pixel which surpasses the anticipated level of uncertainty in any of the derived water and shorelines and the calculated erosion rates. A more accurate Geolocation capability is central to the pre-processing task and is conducted via a coregistration process that will be outlined in later sections. In order to ensure spatial-temporal monitoring of shoreline variability on large scales via satellite imagery provided by several sources and products corrections must be applied. All products must be within the same spatial repository, since the products are characterized by different spatial resolution.

1.1.1 *Information content and quality*

Corrected products will be inter-superimposable images (coregistered images). Every pixel which presents an object or part from a product "A" (Sentinel-2 for example) it will correctly overlap the pixel of the same object which is in the product "B" (from a Worldview image for example). The spatial resolution of the final product will be equivalent to the resolution of the reference product.

1.1.2 *Product Order and delivery services*

Coregistered products will be delivered as a multiband raster (GEOTIFF format), with the filename deriving from the original input image with a suffix detailing the coregistered bands e.g. RGBNIR. Coregistered products will be available to production team to run the different processor, including a metadata file (JSON) which now contains a fully traceable account of the coregistration process including the original reference and target products as well as the key AROSICS processing parameters.

1.2 Feasibility Study

1.2.1 *Satellite sensors and mission*

In this section will be present the most used satellite and sensor for Earth observation studies and analysis. For other EO mission please refer to *Table 1*. This table briefly present mostly used satellite missions in EO projects, with this non-exhaustive list we can see the diversity of sensors available which makes it possible to choose the most adapted to our project.

a. Optical

Passive optical remote sensing sensors measure electromagnetic radiation of different wavelengths reflected from distant objects. Passive optical sensors are day and cloud dependent.

i. High resolution (HR)

Landsat mission marks the beginning of the use of Earth observation satellite data with Landsat 1 launched in July 1972, followed by several optical satellites to improve our knowledge of the Earth. Landsat 5-7 satellites provide high resolution imagery at 30 m resolution from multispectral and thematic mapper sensors for Landsat 5 and from an Enhanced thematic mapper sensor for Landsat 6 and 7. Revisit time: 16 days.

Sentinel-2 mission is a constellation of two polar-orbiting satellites, A and B phased at 180°. Main objective of the mission is to provide global acquisition of high-resolution —10, 20 and 60 meters, multispectral — 13 spectral bands, within 5 days and 2-3 days at mid-latitudes. Sentinel-2 satellites carry an optical instrument payload MSI allowing an optical swath width at 290 km. Coverage limits between latitudes 56° south and 84° north. First Sentinel 2 image: June 2015 from Sentinel -2A.

ii. Very high resolution (VHR)

Worldview 2 is an Earth observation satellite launched in October 2009. It provides high-resolution panchromatic imagery at 0.46 m resolution and multi-spectral imagery at 1.85 m resolution with an average revisit time of 1.1 days. In a single pass, maximum continuous area collectable (30° off-nadir angle) is 138 * 112 km in mono and 63 * 112 km for stereo.

SPOT mission, initiated by the CNES in the 1970s, was designed to improve the knowledge and the management of the Earth. Each satellite up to SPOT4 consists of two imaging instruments acquiring areas of 60*60 km. Panchromatic mode provides black and white image at 10m resolution and multispectral mode which provides 20m colour images acquired simultaneously in three bands (red, green, and near-infrared or medium infrared). SPOT5 satellite consists of two HRG instruments that offer better resolution: 2.5 to 5 meters in panchromatic mode and 10 meters in multispectral mode. Revisit time: 1 day for SPOT 6 & 7.

First PLEIADES satellite, Pleiades 1A, was launched in December 2011 and Pleiades 1B followed in December 2012. Pleiades satellite can image anywhere on Earth in less than 24h at 70 cm resolution in visible and near-infrared spectrum. Pleiades have an extremely sensitive optical instrument that reduces the exposure time needed for each image.

b. Synthetic aperture radar

Radar imagery is an active remote sensing tool, it is both a transmitter and receiver. Radar imagery measures the time of return of the wave between the radar and the ground, the intensity of the received wave and phase shift between the reference of the transmitted wave and the received wave.

Sentinel-1 carries a C- SAR sensor, SAR images (for "Synthetic Aperture Radar") are the result of a complex processing of the raw data, and contain in each pixel, two types of information: the amplitude of the signal backscattered by the ground towards the radar, and its phase. Sentinel-1 mission comprises two polar-orbiting satellites operating day and night. Launched in 2014 and 2016, Sentinel-1 satellites provide imagery in different acquisition mode: Wave mode (WV), interferometric wide swath (IW) and extra wide swath (EW) with a revisit time of 12 days, 6 days for both satellites.

TABLE 1. EO MISSIONS AND THEIR SPECIFICATIONS WITH OPTICAL SENSORS

Satellite constellation	sensor & bands (optical)	pixel resolution of L1 products	Revisit time	Years active
Landsat 7 (ETM+)	0.52 - 0.90 μm	15 m	16 days	1999 – 2020
	0.45 - 0.52 μm , 0.52 - 0.60 μm , 0.63 - 0.69 μm , 0.77 - 0.90 μm	30 m		
Landsat 8 (OLI)	0.503 - 0.676 μm	15 m	16 days	2013 –
	0.435 - 0.451 μm , 0.452 - 0.512 μm , 0.533 - 0.590 μm , 0.636 - 0.673 μm , 0.851 - 0.879 μm	30 m		
Sentinel-2 A & B /MSI	448-546 nm, 537-583 nm, 645-683 nm, 762-908 nm	10 m	5 days	2015 –
	604-723 nm, 731-749 nm, 768-796 nm	20 m		
	430-467 nm, 932-958 nm	60 m		
RapidEye 1,2,3	440–510 nm, 520–590 nm, 630–685 nm, 690–730 nm, 760–850 nm	5 m	1 day	2008 –
Skysat 1...7	Panchro	0.8 m		2013 –
	450-900 nm, 450-515 nm, 515-595 nm, 605-695 nm, 740-900 nm	0.8 m		

Planetscope	610 - 700 nm, 500 - 590 nm, 420 - 530 nm, 770 - 900 nm	3 m		2009-
SPOT 1-2-3-4	0,50-0,73 µm	10 m	5 days	1986 –
	0,50-0,59 µm, 0,61-0,68 µm, 0,78-0,89 µm	20 m		
SPOT5	480 – 710 nm	5 m	2-3 days	2002 –
	500 – 590 nm, 610 – 680 nm, 780 – 890 nm, 1580 – 1750 nm	10 m & 20 m for SWIR		
SPOT6-7	panchro	1.5 m	1 day	2012 –
	0.455-0.525 µm, 0.530-0.590 µm, 0.625- 0.695 µm, 0.760- 0.890 µm	6 m		
Pleiades	480-830 nm	0.7 m	26 days	2009-
	430-550 nm, 490-610, 600-720 nm, 750-950 nm	2.8 m		
Ikonos-2	450-900 nm	0.82 m	1-3 days	2000-
	450 – 530 nm, 520 – 610 nm, 640 – 720 nm, 760 – 860 nm	3.2 m		
Quickbird-2	450 – 900 nm	0.61 m	1-3.5 days	(2001)-2008-2014
	450 – 520 nm, 520 – 600 nm, 630 – 690 nm, 760 – 900 nm	2.4 m		
GeoEye-1	450 – 900 nm	0.41 m	≤ 3 days	2008-
	450 – 510 nm, 520 – 580 nm, 655 – 690 nm, 780 – 920 nm	1.64 m		
WorldView WV-1	400 – 900 nm	0.5 m	1.7-5.9 days	2007-
	450-510 nm, 510-580 nm, 630-690nm, 770-895 nm	-		
WV-2	450-800 nm	0.46 m		2009-
	400-450 nm, 450-510 nm, 510-580 nm, 585-625 nm, 630-690 nm, 705-745 nm, 770-895 nm, 860-1040 nm	1.8 m		
WV-3	450-800 nm	0.31-0.34 m	1 day	2014 –



	400-450nm, 450-510 nm, 510-580 nm, 585-625 nm, 630-690nm, 705-745 nm, 770-895 nm, 860-1040 nm	1.24-1.38 m (MS & VNIR)		
	1195 - 1225 nm, 1550 - 1590 nm, 1640 - 1680 nm, 1710 - 1750 nm, 2145 - 2185 nm, 2185 - 2225 nm, 2235 - 2285 nm, 2295 - 2365 nm	3.7-4.1 m (SWIR)		
	405 - 420 nm, 459 - 509 nm, 525 - 585 nm, 620 - 670 nm, 845 - 885 nm, 897 - 927 nm, 930 - 965 nm,	30 m (CAVIS)		
WV-4	450-800 nm	0.31 m	≤ 4.5 days	2016-2019
	655 - 690 nm, 510 - 580 nm, 450 - 510 nm, 780 - 920 nm	1.24 m		

1.2.2 Existing EO Products

Different products are available for Sentinel-2. Products are a compilation of elementary granules of fixed size along with a single orbit. Granule is the minimum indivisible partition of a product. All data acquired by the MSI will be systematically processed from Level-0 up to Level-1C during the data-reception operation. Level-1C product is orthorectify and provide Top Of Atmosphere (TOA) reflectance. Level-2A prototype product is an orthorectified product providing Bottom-Of Atmosphere reflectance, and basic pixel classification (including cloud).

World view images can be pre-processed with AComp processing for haze and vapor particles removal and is used to correct and clarify high resolution panchromatic and multi-spectral images. Most images are georeferenced to within 5m of their actual location.

SPOT images are not directly usable, pre-processing involves converting the image data into standard SPOT products. Radiometric and geometric corrections are applied according to the level of correction. Level 1A is quite similar to raw data save for radiometric corrections, level 1A products are computed with minimal pre-

processing. Level 1B products includes radiometric and geometric corrections, they are expected to offer a location accuracy of 500m for vertical-viewing and a relative internal error for distance of 0.5×0.001 .

Two processing level have been defined for Pleiades products to fulfil user needs, the sensor level and the ortho-image and mosaic level. Sensor level products are only corrected from on-board radiometric and geometric distortion, no ground projection is operated. The ortho-image and mosaic level products are resampled into a cartographic projection and corrected from sensor and terrain distortion (Baillarin et al, 2010).

The Sentinel-1 mission comprises a constellation of two polar-orbiting satellites, operating day and night performing C-band synthetic aperture radar (SAR) imaging, enabling them to acquire imagery regardless of the weather. Sentinel-1 data come at three levels:

- Level-0. These products consist of the sequence of Flexible Dynamic Block Adaptive Quantization (FDBAQ) compressed unfocused SAR raw data.
- Level-1 data are the generally available products intended for most data users. Level-1 products are produced as Single Look Complex (SLC) and Ground Range Detected (GRD). Level-1 Single Look Complex (SLC) products consist of focused SAR data geo-referenced using orbit and attitude data from the satellite and provided in zero-Doppler slant-range geometry. Level-1 Ground Range Detected (GRD) products consist of focused SAR data that has been detected, multi-looked and projected to ground range using an Earth ellipsoid model.
- Level-2 OCN products include components for Ocean Swell spectra (OSW), a two-dimensional ocean surface swell spectrum, and an estimate of the wind speed and direction per swell spectrum.

1.2.3 *Currently known issues*

It is important to mention that the coregistration module is a module which becomes more resource intensive the moment we use very high-resolution data. If these resources have not satisfied these computing needs, namely the memory where the disk space, several bugs can appear under messages declaring the stop of computation. Generally, it is the kind of problem related to the working environment that often happens, on the other side we can expect problems which are more linked with the image than with anything else, namely:

- **Projection system:** it is essential to recommend using images with the same spatial projection (Reference/Target) and favour the projection system over the coordinate system.

- **No data pixel:** the presence of no data pixels in the image bounds often poses problems during image correction, so a slicing that eliminates these empty pixels is strongly recommended.
- **Cloud cover:** there is not a precise limit linked to the percentage of cloud cover, but the rule here is to have a minimum of reference point on land not covered by clouds, if the rule is not satisfied the process cannot correct the image.

1.2.4 Potential Solutions

The follow-up of a Spatio-temporal event requires the exploitation of information coming from several sensors and in different dates, our challenge is to put all the information in the same frame of reference in order to be able to compare or evaluate the evolution of an event.

Our objective with images coregistration is to be able to treat a temporal series of data while adapting with the change of the spatial precision (resolution) / the quality, whatever the source of information.

1.3 Product Specifications

The processor will generate multiband Geotiff files of any combination that the user requests, with the default being a 4 band RGBNIR product. Sentinel-2 products will be produced at 10m resolution with lower resolution bands being upsampled to 10m. All Landsat-8 bands will be pansharped to 15m resolution prior to coregistration, while earlier Landsat missions will use their standard 30m resolution.

The product name whether it is the Geotiff or the metadata file (Json) will use the following naming convention:

CE_YYYYDDMMHSS_<type>_<category>_<level>_<bbox>_<qualifier>_<YYYYMMDD>.ext

Where the first date is the acquisition date, to the accuracy of a minute, and the end date is optional. The final date is the processing date used to distinguish versions of the same product. The <bbox> is the bounding box of the feature as the latitude and longitude of the lower left and upper right corner. e.g., 411021N014826E-413304N023909E. The <type> is a two-character code 'CR', the <category> a two-character code 'OB' (observation based). The <level> is a two-character code: L1|L2 (single observation). The <qualifier> is used to specify the mission (L5|L8|S2), e.g.

CE_201509101111_CR_OB_L1_502749N030000W-512625N012513W_S2_20201103.tif

2 Algorithm Description

The “AROSICS” (Automated and Robust Open-Source Image Coregistration Software). It is based on a phase correlation approach as proposed by (Foroosh, Zerubia, & Berthod, 2002) and makes use of Fourier shift theorem, enabling the determination of precise X/ Y offsets at a given geographical position. However, phase correlation can only be used for two monochromatic (single band) input images with exactly the same pixel dimensions, representing roughly the same (or slightly shifted) geographical position on the Earth’s surface, ideally also with similar pixel intensity values. This is usually not fulfilled when dealing with multi-temporal and multi-spectral data from different sensors (Figure). Therefore, it was necessary to combine the pure phase correlation approach with additional processing and evaluation modules that are all integrated within the AROSICS framework, representing the intrinsic innovation of the presented work (Scheffler, Hollstein, Diedrich, Segl, & Hostert, 2017).

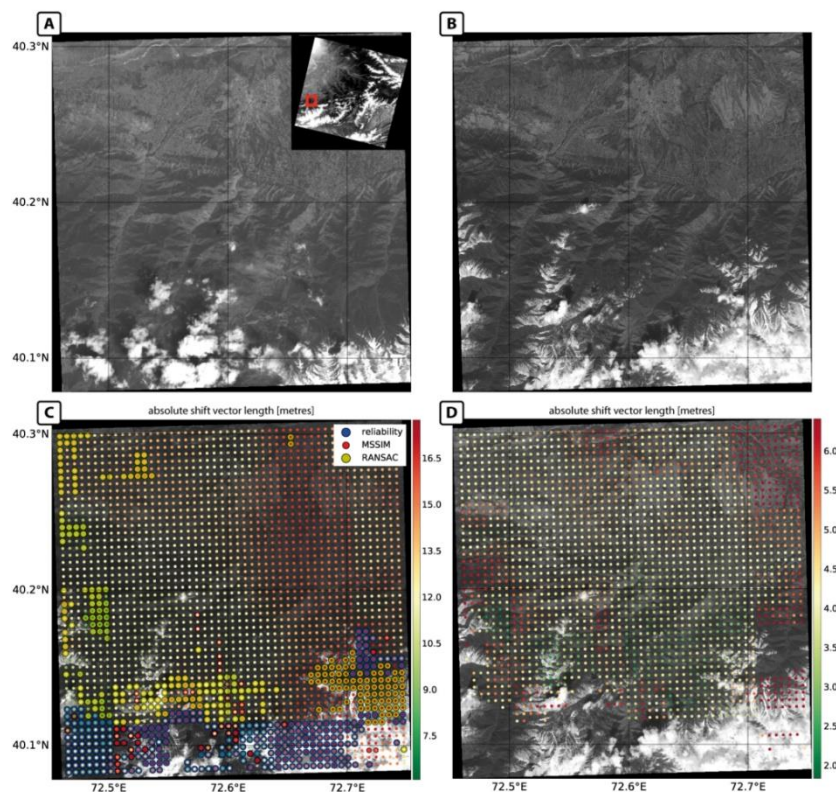


FIGURE 2.1: (A) REFERENCE IMAGE SUBSET (LANDSAT-8, BAND 5), SMALL FIGURE DEMONSTRATES FULL EXTENT; (B) TARGET IMAGE (RAPIDEYE-5, BAND 5); (C) CALCULATED TIE POINT GRID BEFORE CORRECTION (ABSOLUTE SHIFT VECTOR LENGTH IN METRES) INCLUDING FALSE-POSITIVES; AND (D)

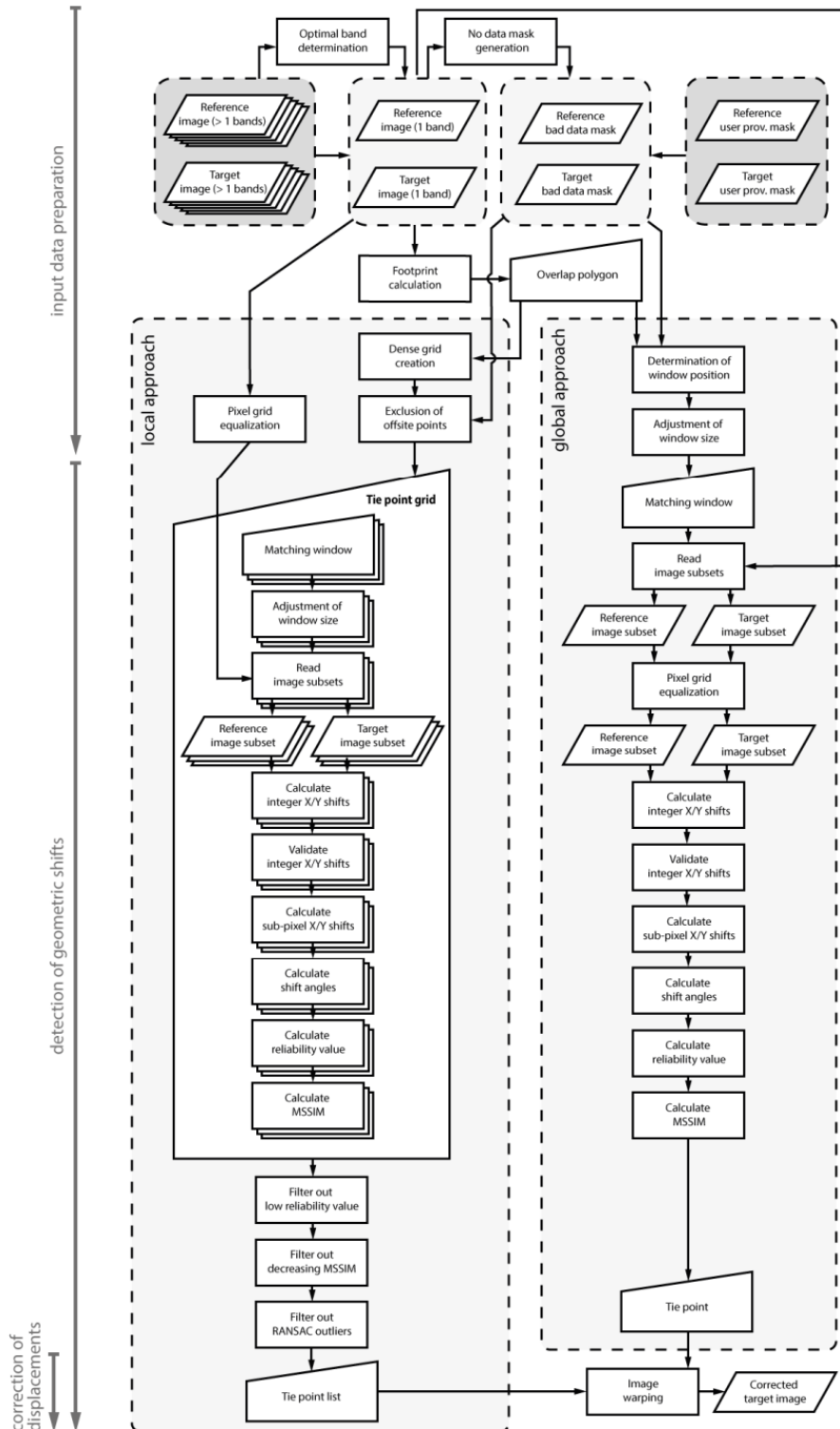


FIGURE 2.2. FLOW CHART OF AROSICS (SCHEFFLER ET AL., 2017)

2.1 Processor Design

The coregistration of a series of satellite images requires adaptation depending on the quality of input images, the most important of which is the resolution of the image. For this we set certain basic considerations to ensure a correct and flexible treatment with the variation of catches in time and space.

Consideration 1 - Reference image selection:

- The reference image must have the better spatial accuracy
- We will start coregistration with recent images and move progressively towards the old images.
- Reference image should ideally be cloud less, but in most cases, we use an image with weak cloud cover only if the clouds no longer hide the fixed reference on earth

Consideration 2 - Image quality:

- Coregistration applied to products of the same sensor gives very satisfactory results, even if the target product is of poor quality, as the calibration process is performed on identical bands
- When the reference and target products are from different sensors, it is essential to have high quality for both products to obtain good results from coregistration as there will be variations in the bandwidths of the two sensors

Based on these two key considerations, we can consider two possible approaches to coregister a batch of HR time series data (Figure).

Scenario-1 - Two levels of coregistration:

1. VHR – VHR: Select a VHR for every 2-5 years and coregister them all to one another
2. VHR – HR : Coregister each HR to the temporally closest VHR from level 1

Scenario-2 - Three levels of coregistration:

1. VHR – VHR: Select a VHR for every 2-5 years and coregister them all to one another
2. VHR – HR: Find the best HR image close to each VHR and coregister
3. HR – HR: Coregister each remaining target HR to the closest reference HR from level 2

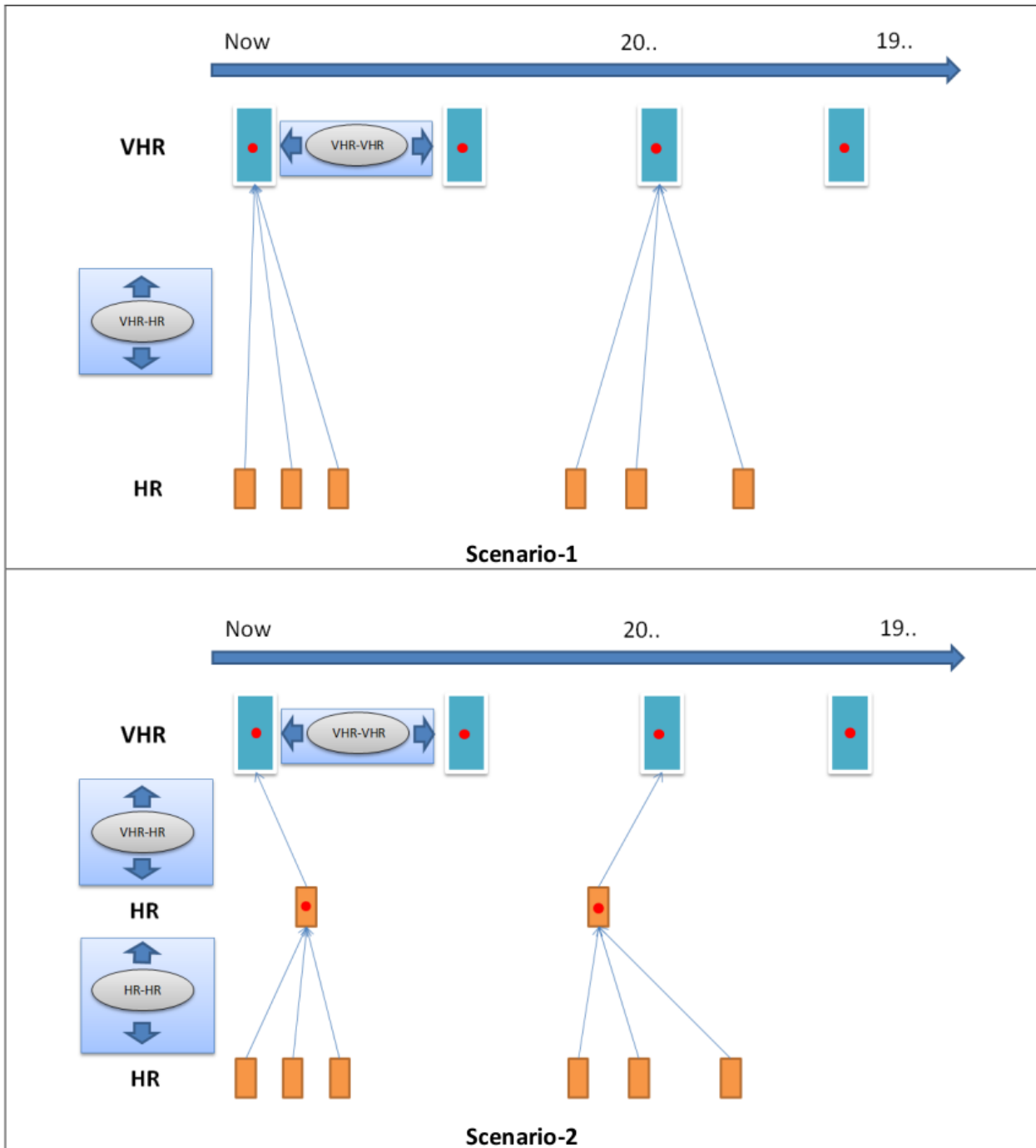


FIGURE 2.3. POSSIBLE SCENARIOS FOR HR COREGISTRATION

The results of the two scenarios are very similar in areas where the products are of good quality, however as described in Consideration 2, there is an improvement in overall coregistration where the quality of target images is inconsistent with Scenario 2. For this reason, scenario 2 is a more reliable system in sites that have significant cloud cover.

2.2 Processor Overview

The coregistration module described in this document runs on top of AROSICS. The module uses an EO product reader developed by ARGANS that reads any optical EO data product e.g. Landsat, Sentinel-2, Pleiades, Aerial Imagery etc. into a standardised data class. This simplifies processing and allows the geolocation module to deal with just a 'Reference' and 'Target' image (**Error! Reference source not found.**), and processes that were manually performed in the previous version such as RGB stacking are now fully automated.

The user as minimum need only supply:

- Reference Product
- Target Product
- Output Directory

However, if a particular combination requires unique parameterisation outside of the default configuration (Table 2) they may also supply a json file containing arguments that are accepted by the AROSICS COREG_LOCAL class e.g. grid resolution, max shift and out resolution.

TABLE 2. AROSICS PARAMETERS FOR EACH LEVEL OF PROCESSING

Case	Composite Band	Grid-res	Max shift	Out resolution
VHR-VHR	Reference-> Composite: 2,3,4	100	20	Lowest resolution in input images
	Target -> Composite: 2,3,4			
VHR-HR	Reference -> Composite: 2,3,4	100	200	Lowest resolution in input images
	Target -> Composite: 2,3,4			
HR-HR	Reference -> Composite: 2,3,4 / All Band	90-100	20	Lowest resolution in input images
	Target -> Composite: 2,3,4 / All Band			

As shown in **Error! Reference source not found.**, an RGB stacked array is produced for the reference and target products which is fed to the AROSICS library which calculates a spatial shift vector between the reference and target. Since all bands in the target product are perfectly aligned this shift can be applied to each band. This stack of shifted target bands is then written to a new geolocated output product.

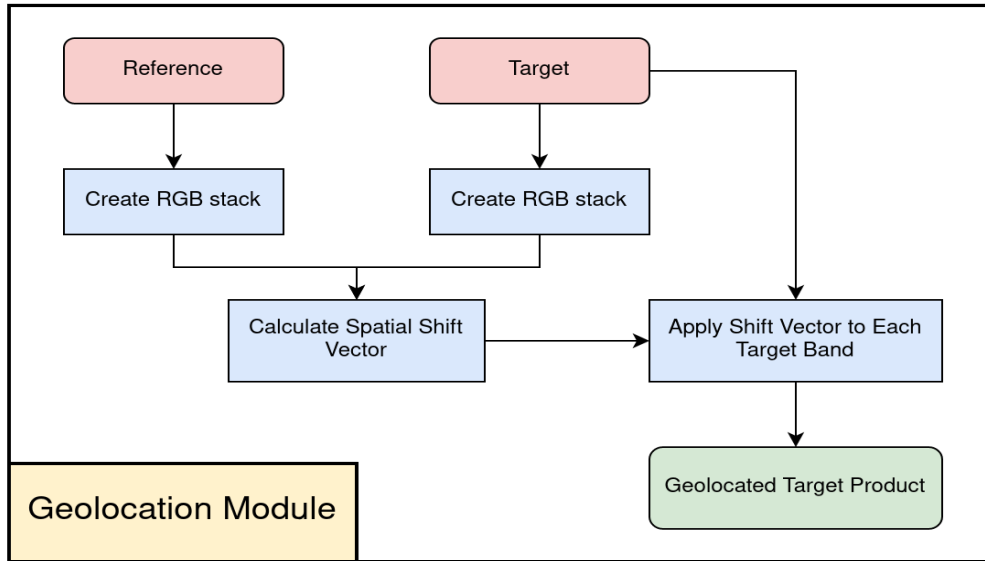


FIGURE 2.4: SCHEMATIC OVERVIEW OF THE GEOLOCATION PROCESSING MODULE

To produce a large time series of geolocated products, the workflow in Figure is used based on the logic of the scenario 2. The geolocation module from Figure Figure 2.4 is instantiated twice. The first time with the VHR product as reference and the highest quality HR, which will become the reference for the rest of the HR, as the target. The second time the georeferenced high-quality HR is instantiated as the reference and the processor iterates through each remaining HR product in the time series.

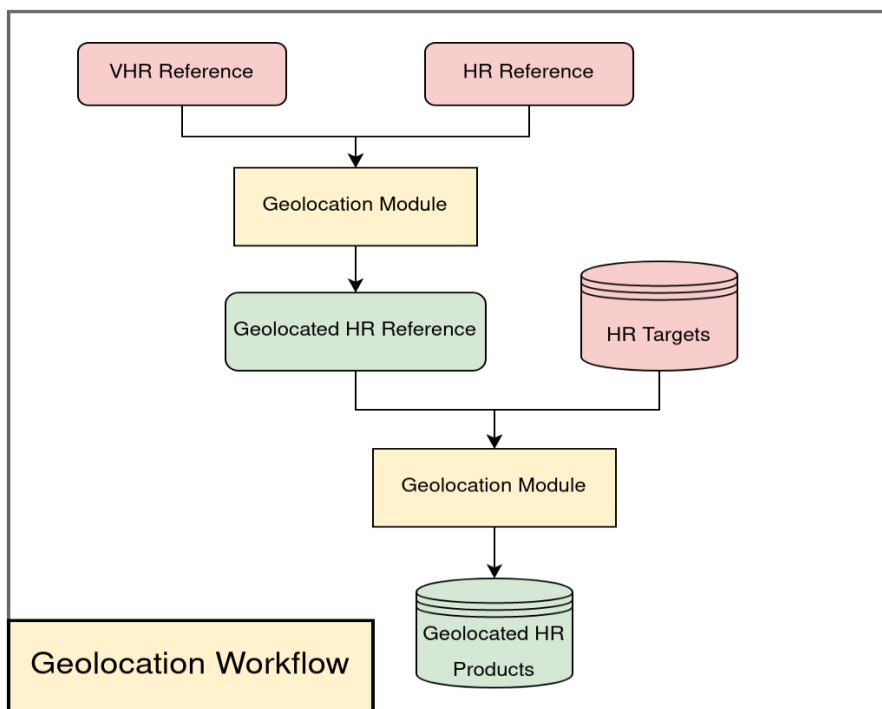


FIGURE 2.5. SCHEMATIC WORKFLOW FOR COREGISTERING A STACK OF HR TARGETS TO A SINGLE VHR

2.3 Data Requirements

The code uses python package to perform automatic subpixel coregistration of two satellite image datasets based on an image matching approach working in the frequency domain, combined with a multistage workflow for effective detection of false positives.

Option used (Local coregistration): A dense grid of tie points is automatically computed, whereas tie points are subsequently validated using a multistage workflow. Only those tie points not marked as false positives are used to compute the parameters of an affine transformation. Warping of the target image is done using an appropriate resampling technique (cubic by default).

For a coregistration to succeed, we should use orthorectified images or images with a low nadir angle (<6%), less deformation implies more luck to successfully coregistration.

- We cannot process images with no data, therefore, in the case of non-square images, the area for coregistration needs to be re-defined.
- For a good quality of coregistration we must have fixed reference objects in the intersection area between the reference image and the target one.

3 Theoretical Description of the Model

3.1 Physical Description

For calculating geometric shifts between the input images within a single matching window, both subset images are transformed into the frequency domain – in this study using FFTW (Fastest Fourier Transform in the West), the fastest freely available implementation of discrete Fourier transform (DFT) that is described in detail by (Frigo & Johnson, 2005). The two resulting images in the frequency domain are phase-correlated to generate their cross-power spectrum, which is then transformed back into spatial domain using inverse FFTW [(Zitová & Flusser, 2003), (Brown, 1992), (Rogass, Segl, Kuester, & Kaufmann, 2013), (Keller, Averbuch, & Israeli, 2005)]. The normalized form of the cross-power spectrum in the spatial domain demonstrates a distinct sharp peak at the point of registration of the input images (Figure 3.1), which can be used for quantification of image displacements [(Zitová & Flusser, 2003), (Leprince, Barbot, Ayoub, & Avouac, 2007), (Foroosh et al., 2002), (Tong et al., 2015)]. Integer shifts can be derived from the distance between the position of the maximum peak and the centre position of the spectrum in the X and Y directions.

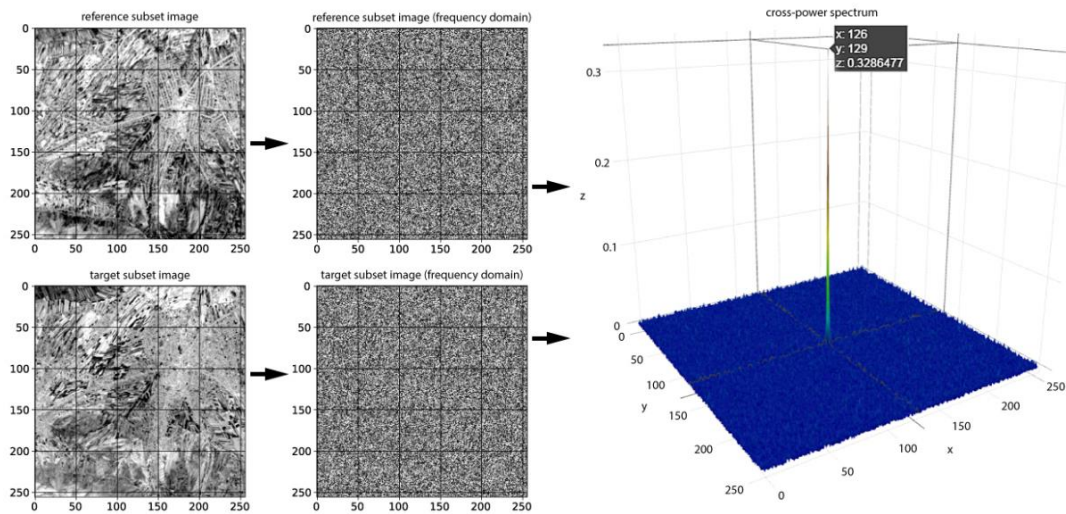


FIGURE 3.1: SUBSET IMAGES WITHIN THE MATCHING WINDOW IN SPATIAL AND FREQUENCY DOMAINS AND THE

3.1.1 5.1.1 Mathematical Description and calculation procedures

The reliability of the X/Y displacements is connected to the pixel value similarity of the input images induced by, e.g., varying illumination or land cover changes or by different sensor noise levels. This is also supported by (Anon 2003; Rogass et al. 2013), and potential effects are quantified by implementing a total of five complementary validation techniques. Their individual performance depends on the image content of the input images and the pattern of misregistration. They build upon each other and aim to avoid different sources of erroneous shift detection but may also be deactivated on demand.

However, optimal validation results have been observed by combining the following validation techniques:

- 1- Validity check of the calculated integer shifts has been implemented.
- 2- Threshold check
- 3- Reliability filtering.
- 4- Structural Similarity Index (MSSIM).
- 5- RANSAC (algorithm).

3.1.2 5.1.2 Acceptance of the Models

Various aspects must be considered when comparing the overall performance of the process framework with existing state of the art coregistration workflows. From the pure perspective of registration accuracy, the

implemented algorithm based on (Feroosh et al. 2002) achieves accuracies better than $1e^{-3}$ pixel (Relative unit linked with the image to be corrected, Example: S2: 10m / L8: 15m / L5: 30 m) in most scenarios (Rogass et al. 2013), which is an excellent result compared with, e.g., 2D Gaussian peak fit (Nobach and Honkanen 2005), achieving $1e^{-1}$ pixel under optimal conditions (Rogass et al. 2013). However, this may be easily outperformed by other techniques, e.g., those proposed by (Averbuch and Keller 2002) or (Rogass et al. 2013), allowing for accuracies up to $1e^{-6}$ pixel (Rogass et al. 2013). However, these values only apply for global coregistration at high SNR conditions. In case of local coregistration featuring image, warping based on affine transformation parameters, deviations from the affine model, e.g., caused by topographic effects, decrease registration accuracy. Nonetheless, the intention of the proposed algorithm is not primarily to outperform existing coregistration accuracies but rather to achieve a high level of automation and robustness, coupled with generic and operational applicability while reliably reaching local coregistration accuracy in the sub-pixel range.

3.1.3 5.1.3 Error estimation

For local coregistration, the AROSICS framework achieved root mean square errors of 0.3, 0.15 and 0.32 pixels using an affine transformation model. (Yan et al. 2016) achieved 0.286, 0.302 and 0.303 pixels for three Landsat-8 and Sentinel-2A image pairs in case of affine transformation and showed that a polynomial transformation could not significantly improve these results. Regarding computational speed in case of global coregistration, (Rogass et al. 2013) compared the implemented phase correlation (Feroosh et al. 2002) method with: (1) their own coregistration algorithm; (2) a Fourier based approach proposed by (Averbuch and Keller 2002); and (3) with 2D Gaussian peak fit (Nobach and Honkanen 2005). The approach of (Feroosh et al. 2002) outperformed them. However, the computational load for local coregistration mainly depends on the required number of tie points for coregistration and is therefore directly connected to the complexity of misregistration.

3.1.4 5.1.4 Algorithm output

Coregistered products will be delivered as a multiband raster (GEOTIFF format). Coregistered products will be available to production team to run the different processor, including a metadata file (JSON) which now contains a fully traceable account of the coregistration process including the original reference and target products as well as the key AROSICS processing parameters.

3.2 Algorithm Performance Estimates

A comparison of root mean square (RMSE) errors of detected displacements before and after the correction was conducted to quantitatively assess the overall performance of the proposed coregistration workflow. Figure demonstrates the detected shift distributions before and after correction for the use cases INTER1, INTER2 and INTRA2. Green markers show valid TPs, whereas red markers stand for false positives. The indicated RMSE values were calculated based on all absolute X/Y shifts within the whole tie point grid, after the exclusion of false-positives (Scheffler et al., 2017).

Tests have been applied on an S2 image (as target), the reference one was selected from the same satellite product with a spatial resolution of 10 m. After the definition of input path and the output one, and we've executing the code. Figure 3.4 shows a comparison between status before and after the coregistration, to see the difference we have using a small circle area inside the pixel. For this case of study, the results of comparison show that we have a small a displacement of 10 m (by one pixel).

Name	Reference/Target Image (R/T)	Sensor	Acquisition Date	Spatial Resolution (m)	Image Dimensions (Rows, Columns)	Processing Level
INTER1	R	Landsat-8, band 2	<multiple>	15	7320, 7320	1T
	T	Sentinel-2A, band 3	29 May 2016	10	10,980, 10,980	1C
INTER2	R	Landsat-8, band 5	1 June 2013	30	7541, 7721	1T
	T	RapidEye, band 5	23 April 2013	5	5000, 5000	3A
INTRA1	R	Sentinel-2A, band 7	11 January 2017	20	5490, 5490	1C
	T	Sentinel-2A, band 8A	11 January 2017	20	5490, 5490	1C
INTRA2	R	TerraSAR-X, X-band	10 February 2014	2.75	19,090, 15,636	EEC
	T	TerraSAR-X, X-band	1 January 2015	2.75	19,090, 15,636	EEC

FIGURE 3.2. SUMMARY OF EXAMPLE SATELLITE DATASETS

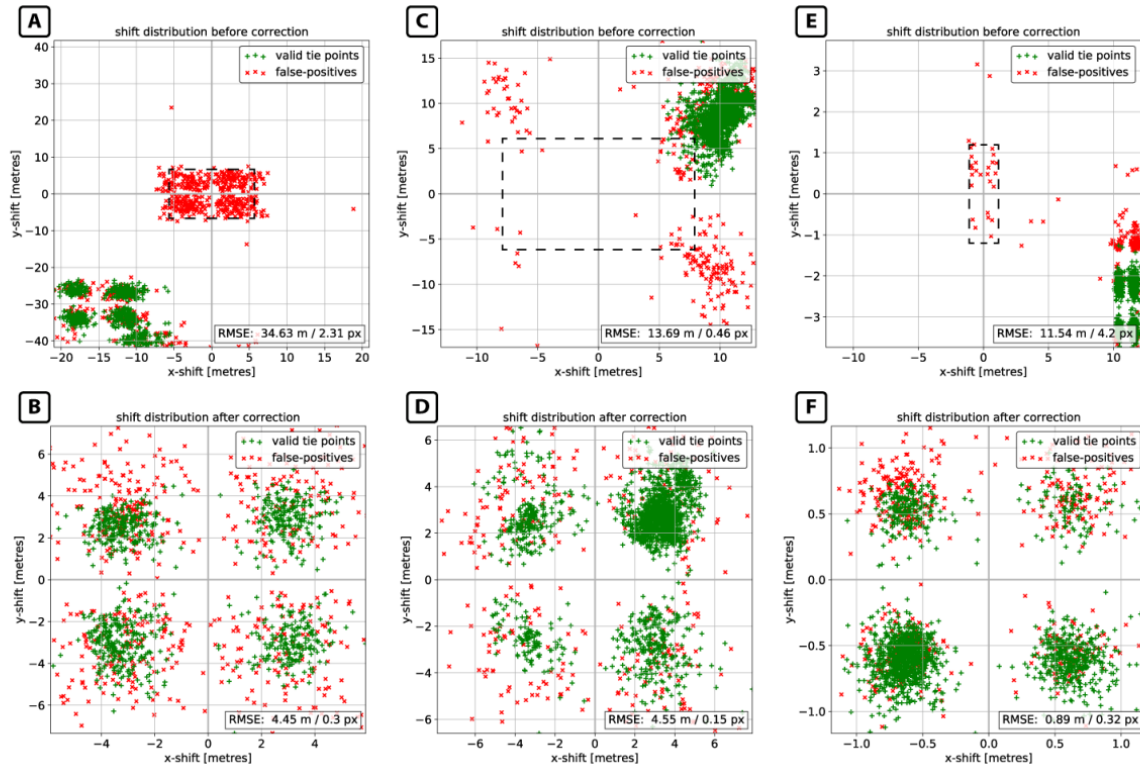


FIGURE 3.3. DISTRIBUTION OF DETECTED GEOMETRIC SHIFTS BEFORE AND AFTER CORRECTION. RMSE IN PIXEL UNITS ALWAYS REFERS TO THE SPATIAL RESOLUTION DURING IMAGE MATCHING: (A,B) USE CASE INTER1—SENTINEL-2/LANDSAT-8; (C,D) USE CASE INTER2—RAPID-EYE-5/LANDSAT-8; AND (E,F)

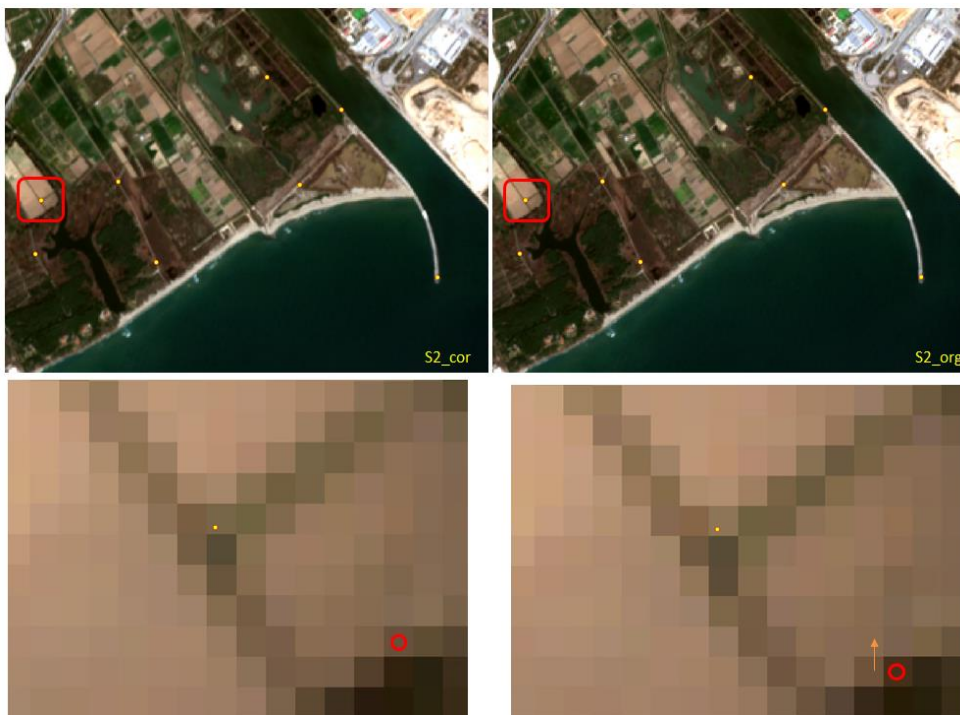


FIGURE 3.4. TOP: IMAGE LARGE SCALE BOTTOM: ZOOM), LEFT SIDE: AFTER COREGISTRATION / RIGHT SIDE: IMAGE ORIGINAL, ARROW (DIRECTION OF DISPLACEMENT)

3.3 Product Validation

The Coregistration is considered as a relocation of an image compared to another supposed to be correct (This means that my reference image must be a good reference on the level of position and precision). The module used validates the possibility of coregistration according to the number and the quality of the points of similarity between the two images. In the case where coregistration is not possible, no results are left.

3.3.1 Test specifications

The validation test is based on the use of the metadata resulting from the coregistration, specifically the parameter SSIM (Structural similarity index) which makes it possible to measure the similarity between two images in a way closer to human subjective perception than the 2 metrics (contrast term and structure term). It is based on the observation that human vision is strongly adapted to the analysis of structural information and therefore aims to effectively measure the alterations of this information between the source image and the target image.

It is the product of 2 components: a contrast term (changes in contrast, gamma distortion), and a structure term (blur, noise, posterization, accentuation).

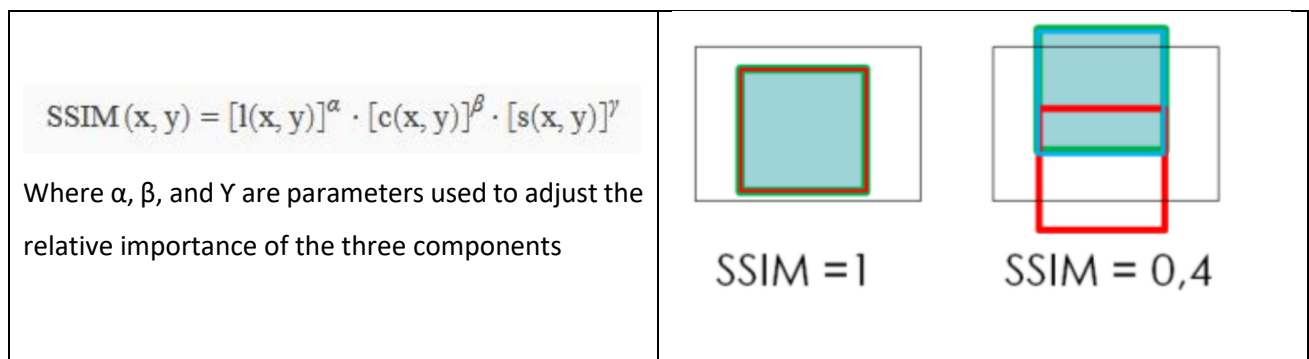


FIGURE 3.5. EQUATION FOR SSIM INDEX

3.3.2 Test Datasets

We used two sentinel data images (2016 /2018) with different atmospheric conditions (one clear and the other cloudy) to check if they impacted the quality of coregistration. This information can help us to evaluate the stability of the coregistration process during a long period.

Two levels have been adopted to carry out this quality control.

- Level 1: the quality control for this level consists in making a comparison of the variation of the index (SSIM) before and after the coregistration, in order to see if there is an improvement related to the relocation of the picture, this test was carried out for both dates.
- Level 2: At this stage, we try to verify the stability of the model used 'coregistration' in a time series by evaluating the correlation rate between the indexes after coregistration of two different dates using the same image of reference.

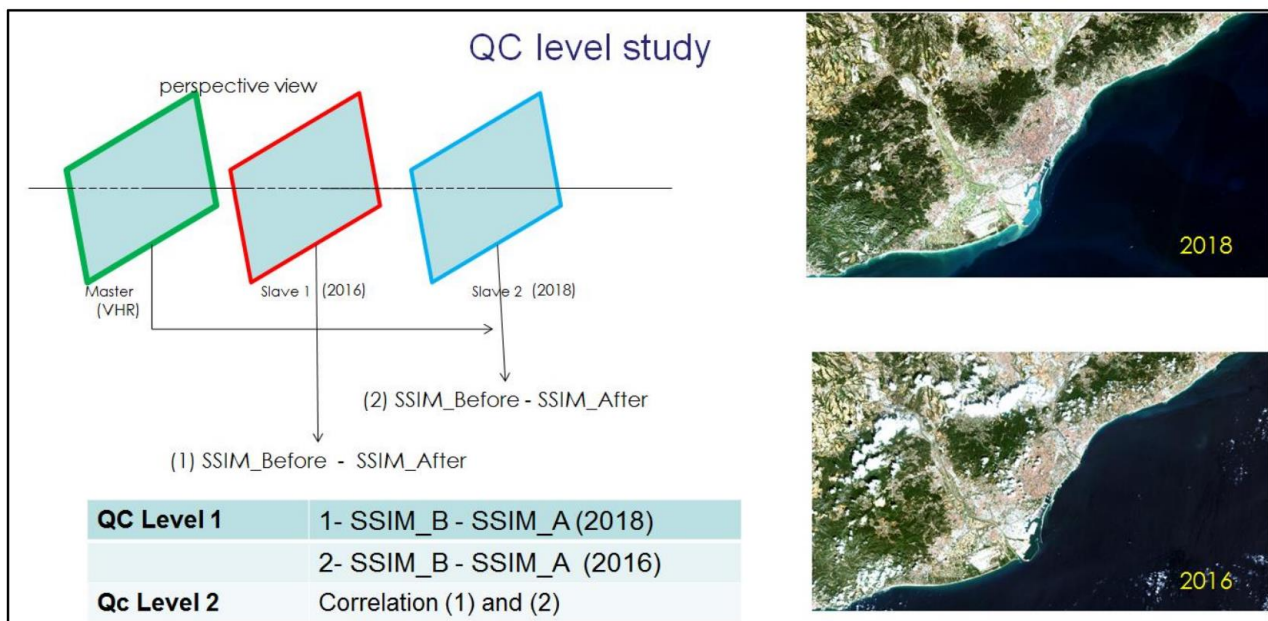


FIGURE 3.6. QUALITY CONTROL (LEVEL OF VALIDATION)

3.3.3 Validation Level 1

The geolocation improvement for a set of images is established using a SSIM index approach. The history of quality changes before and after the model application allows us to visualize the improvement with two scales of measurement.

1. Statistical analysis of 'Percentile 90':

The graph in Figure presents a point cloud which is the result of intersection between the axis of the values of SSIM index and that of the number pixel number (ID), before and after the coregistration for the two dates. The changes will be detected on the Y axis. Between the different profiles we can notice that there is a positive evolution between the situation before and after the coregistration. This change was quantified by calculating percentile 90, which gives an indication of the dominant situation.

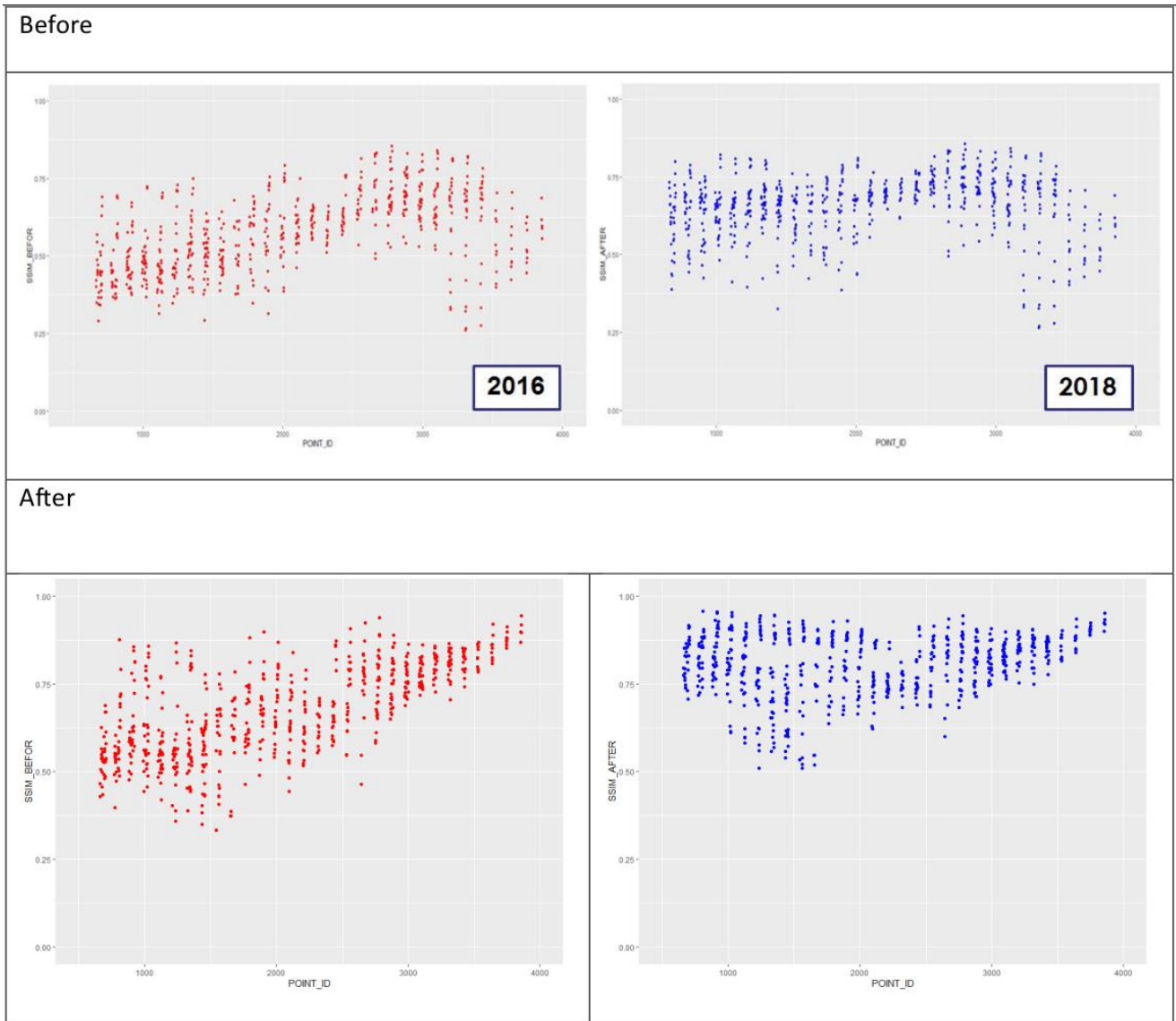


FIGURE 3.7. ANALYSIS OF THE SIM INDEX (BEFORE AND AFTER) THE COREGISTRATION FOR TWO DIFFERENT DATES

This statistical value shows the difference between the quality of the image 2018 (clear) and the image 2016 (cloudy), since the value of first is 'excellent' following (the index) while the other is judged 'well'. The coregistration allowed increasing the image quality to 6.6% while for the second a value of 4.1% was recorded.

TABLE 3. SSIM COMPARISON PRE AND POST COREGISTRATION

Product	90 th Percentile	Improvement
B2018	84%	6.6%
A2018	90%	
B2016	73%	4.1%
A2016	77%	

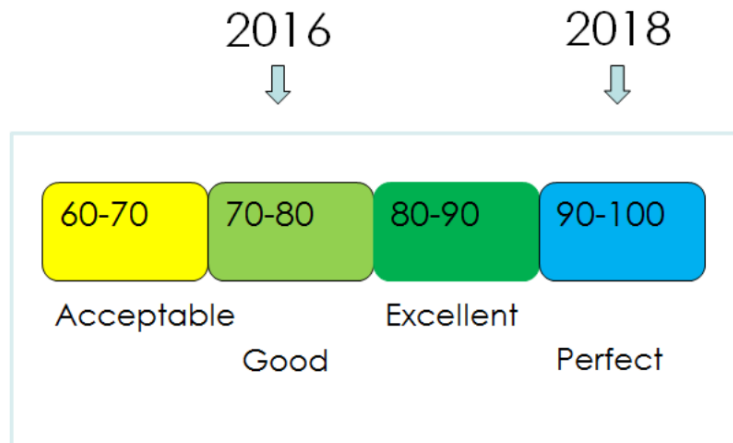


FIGURE 3.8. COREGISTRATION QUANTIFICATION

2. Change compared to the average:

In relation to this reference, it is clear that after geolocation all the points which are below this limit have completely passed to the upper level (Figure).

3. Change in relation to the 70% and 100% interval:

Before the correction of the image, notice that this interval was almost empty (5% of the points in this interval), unlike the state after where the majority of the points are located in the interval 70% -100% (Figure).

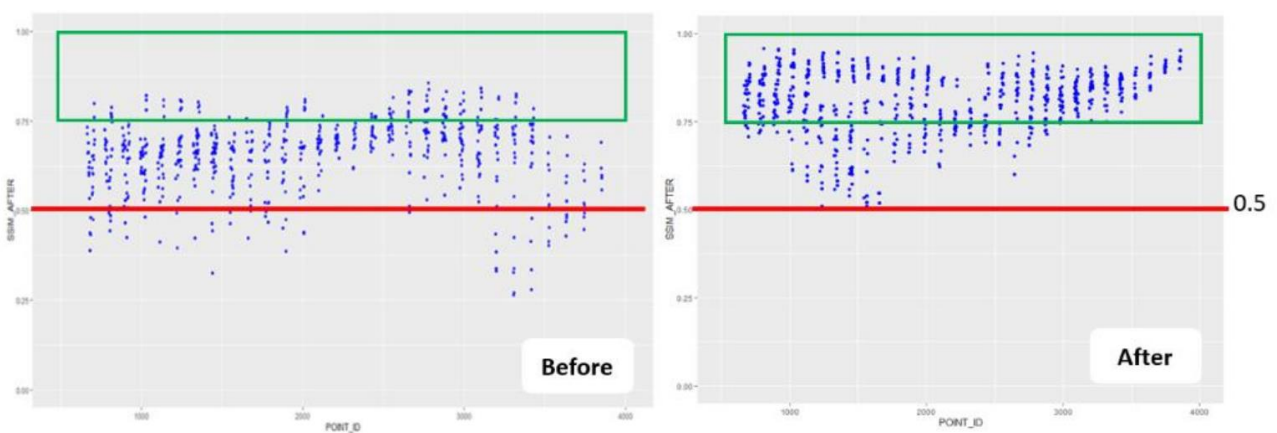


FIGURE 3.9. SSIM INDEX COMPARISON BEFORE AND AFTER THE COREGISTRATION PROCESS

3.3.4 5.3.4 Validation Level 2

The second level of confirmation consists in having a second confirmation that an object x of date 1 which moved (corrected) corresponds to the same object x of date 2 corrected as well. It's coming back confirmed that the SSIM value (date1) of pixel X matches or is close to SSIM (date 2). In this logic we calculated the correlation between the SSIM values of the date 2016 and 2018, the results show a very strong correlation between the two dates.

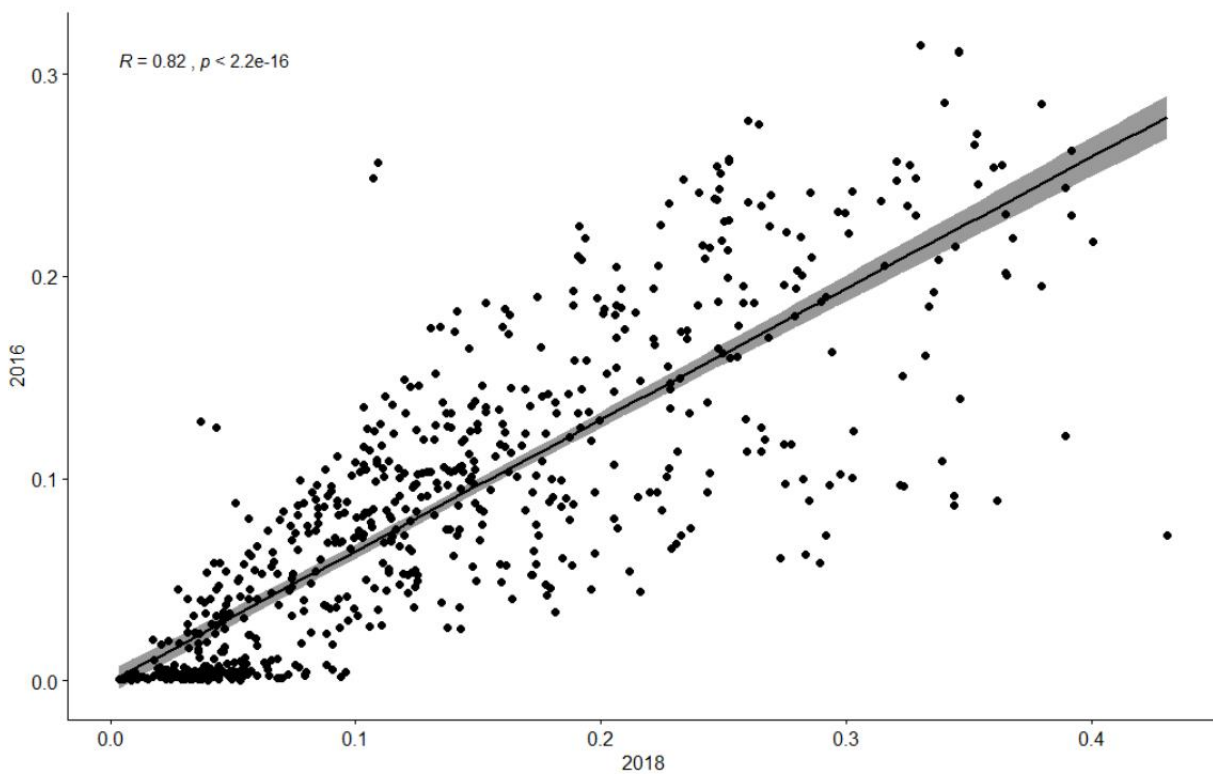


FIGURE 3.10. CORRELATION STUDY OF THE SSIM INDEX BETWEEN THE 2016 AND 2018 IMAGE

4 Refactoring

4.1 Verification

To verify that the refactored processor could be used to replace to the original version a series of test locations were examined. The aim of this was to demonstrate any variations in the final coregistered product. 12 sites were selected across 4 different Sentinel-2 tiles that had been coregistered to Pleiades imagery. User defined polygons were drawn around features in both the original coregistered product and the new version that were:

- Low lying, ideally flat, to avoid shifts due to off nadir angles
- Spectrally stable

Coregistration results were nearly identical as shown by results in Figure to **Error! Reference source not found.** Across the tested locations, variations between the two coregistered products were always subpixel (<10m for Sentinel-2). As shown in Table 4, SSIM values increased in all instances especially in tile T33TUL where the original SSIM value of the product was well below the minimum threshold for an acceptably coregistered product.



FIGURE 4.1. ITALY T33TUL. ORIGINAL COREGISTERED POLYGON IN RED AND REFACTORED VERSION IN BLUE



FIGURE 4.2. ITALY T33SWB. ORIGINAL COREGISTERED POLYGON IN RED AND REFACTORED IN BLUE

TABLE 4. SSIM COMPARISON AT THE 90TH PERCENTILE

	T33TUL	T33SWB	T17XNA
Pre-coregistration	47%	76%	73%
Post-coregistration	62%	81%	79%
Improvement	15%	5%	6%

4.2 Processing Time Improvement

The processing time has been considerably improved for all processes (Table 5). Full band coregistration was the previous default behaviour, however with the refactored version the user can request only the bands of interest to them and their project. As such an RGBNIR product is available in considerably less time, which saves both reduces computational expense and storage requirements.



TABLE 5. COREGISTRATION PROCESSING TIMES

	Original Full Band	Refactored Full Band	Refactored RGBNIR
VHR – HR	10-15 mins	< 5 mins	< 2 mins
HR – HR	~5 mins	< 4 mins	< 3 mins

4.3 Metadata

To ensure full traceability and repeatability of coregistered products, an accompanying metadata JSON file is produced with every coregistered output (Table 6). This file contains the details the version of the processor and the two main packages that it relies upon: AROSICS and ProductReader (internal ARGANS package). Along with this information, the reference and target files and the bands used from each to calculate the geometric shift are recorded. Any non-default AROSICS parameters, that the user may configure in the config file, are also recorded.

TABLE 6. METADATA PRODUCED FOR EACH COREGISTERED PRODUCT

		Example Values
GeneralInfo	ProductName	S2A_MSIL2A_20170717T113321_N0205_R080_T29UPV_20170717T113326_RGBNIR.tif
	ProductDescription	Coregistered Image
	ProductType	CR
	ProductCategory	OB
	LastModifiedDate	20220810
Processor	ProcessorName	Arosics_CE
	ProcessorVersion	CR_0.2.0
	AROSICSVersion	1.2
	ProductReaderVersion	0.0.7
	ProcessingDateTime	20220810T120112
	ProducedBy	jsmith
	ProductionFacility	ARGANS Ltd.
InputData	ReferenceFilename	PL1_OPER_HIR_PMS_3_20130427T114700_N53-481_W006-131_2061.SIP

TargetFileName	S2A_MSIL2A_20170717T113321_N0205_R080_T29UPV_20170717T113326.SAFE
ReferenceBands	"B01", "B02", "B03"
TargetBands	"B02", "B03", "B04"
grid_res	200
max_shift	20
out_gsd	[10., 10.]
nodata	(0, 0)

5 Conclusion

Within the framework of this project, the reduction of the offset error between the images is among the important tasks in the processing chain which is now possible thanks to the coregistration module used. Thanks to the coregistration techniques used to reduce errors due to relative alignment between images, the final rendering quality has been further improved, whether for shoreline tracking or other tasks. With the presence of an acceptable cloud rate, or with different scene lighting, the geolocation tests performed show a positive improvement after the correction, up to 3m of spatial accuracy for Sentinel-2 data. These tests are mainly based on the analysis of the similarity index before and after the coregistration when evaluating a single image, and on the correlation study for the model stability study for a series of imaging. For the first level (study of a single image) the corrected image records a clear improvement in the index compared to the statistical mean and a majority improvement in relation to the interval located between percentile 70 and 100, for model stability over a time series (level two) the correlation recorded a significant value of around 89%.

The refactored processor has improved processing times, while maintaining the same high standard of geolocation accuracy. This has helped to reduce the computational cost that was highlighted as one of the key issues with the first iteration of the processor. Furthermore, the processor itself has been simplified both in terms of the code base and the requirements for the user, and a metadata file detailing the complete parameterisation of the coregistration process is now produced with each file to ensure complete traceability and replicability of each output product.

6 References

- Baillarin S. & Panem C. Pleiades-HR imaging system: Ground processing and products performances. in XXXVIII, Part 7B, (Wagner W., Székely, B., 2010).
- Brown, L. G. (1992). A Survey of Image Registration Techniques. *ACM Comput. Surv.*, 24(4), 325–376.
<https://doi.org/10.1145/146370.146374>
- Foroosh, H., Zerubia, J. B., & Berthod, M. (2002). Extension of phase correlation to subpixel registration. *IEEE Transactions on Image Processing*, 11(3), 188-200. <https://doi.org/10.1109/83.988953>
- Frigo, M., & Johnson, S. G. (2005). The Design and Implementation of FFTW3. *Proceedings of the IEEE*, 93(2), 216-231. <https://doi.org/10.1109/JPROC.2004.840301>
- Keller, Y., Averbuch, A., & Israeli, M. (2005). Pseudopolar-based estimation of large translations, rotations, and scalings in images. *IEEE Transactions on Image Processing*, 14(1), 12-22.
<https://doi.org/10.1109/TIP.2004.838692>
- Leprince, S., Barbot, S., Ayoub, F., & Avouac, J.-P. (2007). Automatic and Precise Orthorectification, Coregistration, and Subpixel Correlation of Satellite Images, Application to Ground Deformation Measurements. *IEEE Transactions on Geoscience and Remote Sensing*, 45(6), 1529-1558.
<https://doi.org/10.1109/TGRS.2006.888937>
- Rogass, C., Segl, K., Kuester, T., & Kaufmann, H. (2013). Performance of correlation approaches for the evaluation of spatial distortion reductions. *Remote Sensing Letters*, 4(12), 1214-1223.
<https://doi.org/10.1080/2150704X.2013.860565>
- Scheffler, D., Hollstein, A., Diedrich, H., Segl, K., & Hostert, P. (2017). AROSICS : An Automated and Robust Open-Source Image Co-Registration Software for Multi-Sensor Satellite Data. *Remote Sensing*, 9(7), 676. <https://doi.org/10.3390/rs9070676>



- Tong, X., Ye, Z., Xu, Y., Liu, S., Li, L., Xie, H., & Li, T. (2015). A Novel Subpixel Phase Correlation Method Using Singular Value Decomposition and Unified Random Sample Consensus. *IEEE Transactions on Geoscience and Remote Sensing*, 53(8), 4143-4156. <https://doi.org/10.1109/TGRS.2015.2391999>
- Zitová, B., & Flusser, J. (2003). Image registration methods : A survey. *Image and Vision Computing*, 21(11), 977-1000. [https://doi.org/10.1016/S0262-8856\(03\)00137-9](https://doi.org/10.1016/S0262-8856(03)00137-9)



End of Document